processes

MDPI

Article

Adsorptive Removal of Boron by DIAION™ CRB05: Characterization, Kinetics, Isotherm, and Optimization by Response Surface Methodology

Baker Nasser Saleh Al-dhawi [1,*], Shamsul Rahman Mohamed Kutty [1], Gasim Hayder [2,3,*], Bushra Mohamed Elamin Elnaim [4], Mohammed Mnzool [5], Azmatullah Noor [1], Anwar Ameen Hezam Saeed [6], Najib Mohammed Yahya Al-Mahbashi [1], Ahmed Al-Nini [1] and Ahmad Hussaini Jagaba [1,7]

[1] Department of Civil and Environmental Engineering, Universiti Teknologi PETRONAS, Bandar Seri Iskandar 32610, Perak Darul Ridzuan, Malaysia
[2] Department of Civil Engineering, College of Engineering, Universiti Tenaga Nasional (UNITEN), Kajang 43000, Selangor Darul Ehsan, Malaysia
[3] Institute of Energy Infrastructure (IEI), Universiti Tenaga Nasional (UNITEN), Kajang 43000, Selangor Darul Ehsan, Malaysia
[4] Department of Computer Science, College of Science and Humanities, Al-Sulail, Prince Sattam Bin Abdulaziz University, Al-Kharj 16278, Saudi Arabia
[5] Department of Civil Engineering, College of Engineering, Taif University, Taif 21944, Saudi Arabia
[6] Department of Chemical Engineering, Universiti Teknologi PETRONAS, Bandar Seri Iskandar 32610, Perak Darul Ridzuan, Malaysia
[7] Department of Civil Engineering, Abubakar Tafawa Balewa University, Bauchi 740272, Nigeria
* Correspondence: bakeraldhawi@gmail.com (B.N.S.A.-d.); gasim@uniten.edu.my (G.H.)

Abstract: A significant issue for the ecosystem is the presence of boron in water resources, particularly in produced water. Batch and dynamic experiments were used in this research to extract boron in the form of boric acid from aqueous solutions using boron selective resins, DIAION CRB05. DIAION™ CRB05 is an adsorbent that is effective in extracting boron from aqueous solutions due to its high binding capacity and selectivity for boron ions, and it is also regenerable, making it cost-effective and sustainable. Field Emission Scanning Electron Microscopy (FESEM), X-ray diffraction (XRD), and FTIR analysis for DIAION CRB05 characterization. To increase the adsorption capacity and find the ideal values for predictor variables such as pH, adsorbent dose, time, and boric acid concentration, the Box–Behnken response surface method (RSM) was applied. The dosage was reported to be 2000 mg/L at pH 2 and boron initial concentration of 1115 mg/L with 255 min for the highest removal anticipated from RSM. According to the outcomes of this research, the DIAION CRB05 material enhanced boron removal capability and has superior performance to several currently available adsorbents, which makes it suitable for use as an adsorbent for removing boric acid from aqueous solutions. The outcomes of isotherm and kinetic experiments were fitted using linear methods. The Temkin isotherm and the pseudo-first-order model were found to have good fits after comparison with R^2 of 0.998, and 0.997, respectively. The results of the study demonstrate the effectiveness of DIAION™ CRB05 in removing boron from aqueous solutions and provide insight into the optimal conditions for the adsorption process. Thus, the DIAION CRB05 resin was chosen as the ideal choice for recovering boron from an aqueous solution because of its higher sorption capacity and percentage of boron absorbed.

Keywords: boron; adsorption; kinetic studies; response surface methodology; DIAION CRB05 resin

check for updates

Citation: Al-dhawi, B.N.S.; Kutty, S.R.M.; Hayder, G.; Elnaim, B.M.E.; Mnzool, M.; Noor, A.; Saeed, A.A.H.; Al-Mahbashi, N.M.Y.; Al-Nini, A.; Jagaba, A.H. Adsorptive Removal of Boron by DIAION™ CRB05: Characterization, Kinetics, Isotherm, and Optimization by Response Surface Methodology. *Processes* **2023**, *11*, 453. https://doi.org/10.3390/pr11020453

Academic Editor: Monika Wawrzkiewicz

Received: 8 January 2023
Revised: 28 January 2023
Accepted: 30 January 2023
Published: 2 February 2023

1. Introduction

As a natural element, boron is found naturally in water bodies, particularly seawater. It is generally regarded as a necessary component of plants, animals, and humans in significant controlled quantities. Excessive boron concentrations in water bodies are

primarily caused by man-made pollution, the majority of which is found in surface water, groundwater, and water bodies [1,2]. Borate (BO_3) is classified as a halogen that causes high levels of saturated acetate in surface water and is mainly released by wastewater containing large quantities of detergents that involve borate (BO_3). Additionally, industrial waste, including chemical additives, plastic bottle, and fertilizers contribute significantly to water pollution through boron [3]. Because of this soil leaching and sedimentary rocks, groundwater contains borate and borosilicate, which are chemical forms of B [4]. Boron concentrations in surface and groundwater typically range from 4.5 mg/L to 100 mg/L, respectively [5,6]. It is frequently used in a variety of products, including glass, weatherproofing wood against flames, cosmetics, soap, detergent, catalysts, and soil fertilizers for deficient soil [7]. Boron, in small amounts, plays an important role in plant growth and crop yield [8]. In contrast, boron B at high concentrations may be harmful to plants, animals, and humans. B concentrations vary significantly in geothermal sources [9].

Furthermore, boron minerals do react with geothermal water, thereby harming the environment. However, the release of boron B via the aforementioned sectors does contaminate water supplies. The recommended limit for boron in drinking water set by the World Health Organization (WHO), is 2.4 mg/L; however, the European Union (EU) has a lower recommendation of 1 mg/L [10,11]. It is essential to conduct a more thorough treatment to guarantee that the boron concentration is within the safe range. V. Vallès et al. found that boron was effectively removed from the solution using N-Methylglucamine sorbents, with a sorption rate of greater than 98%. N-Methylpyridine sorbents were also able to sorb B, with a sorption rate of 75%. Desorption of B from N-Methylglucamine sorbents was between 37–64%, while desorption from N-Methylpyridine sorbents was between 66–99% [12]. There has been a significant amount of research on techniques for removing boron from water, including methods such as electrocoagulation, ion exchange, reverse osmosis, and adsorption. Among these techniques, adsorption has become a popular choice for boron removal due to its ease of use, consistent removal effect, and wide range of applications. Currently, various adsorption materials have been developed for boron removal, including nano-scale materials, activated carbon, and chelating resins. However, most of the research has focused on removing high concentrations of boron from wastewater and not enough on lower levels of boron commonly found in produced water. Therefore, there is a need for a new type of adsorbent that is more effective at removing lower concentrations of boron [13–16]. However, adsorption has been the popular method due to its ease of use, safety, and low cost [17]. When the literature was examined, it was discovered that amberlite resins, such as amberlite IRA743 resin, were competitive adsorbents for boron removal. Adsorbents such as magnetite nanoparticles (Fe_3O_4), metal–organic frameworks, various clays, and MgO have recently been reported to be effective for boron removal [18–21]. Boron is discovered in a neutral in shape of $(B(OH)_3$ in the pH of seawater naturally, as a result, boron selective ion exchange (IEX) resins are thought as the ideal method for extracting boron [22,23].

Several researchers have suggested the use of IEX resins to remove boron from liquid streams. It is worthwhile to highlight the work of Jung and Kim that evaluated the application of the boron selective DIAION CRB05 for seawater boron extraction (boron concentration of approximately 4.4 mg/L) [24]. According to the researchers, boron B sorption rates were 95% and extraction rates were 87%. Yoshizuka and Nishihama investigated the extraction of boron from geothermal water utilizing selective resins CRB03 and CRB05 and Chelest Fiber [25]. A 15 mg/L boron concentration was found in the geothermal water obtained at Obama Hot Spring (Japan). For CRB03 85%, 88% for CRB05, and 99.8% for Chelest Fiber, the boron recoveries were achieved. Additionally, M. Figueira et al. suggested a technique for the boron separation and purity for isotopic analysis of boron in natural sources Initially, boron was recovered from the samples using a column filled with amberlite IRA743 selective resin for boron. The samples were removed with HCl and then moved via a column of mixed IEX resins (Dowex50Wx8 and Ion Exchanger II) that absorbed the HCl as well as the other cations and anions still present within the

eluant, except for boron. Between 91.6% and 102% of the boron was extracted using this method. On the other hand, this most recent work did not concentrate on recovering a sizable amount of boron for commercialization, but rather on purifying boron in natural samples for isotopic analysis [26].

To be able to commercially recover boron using a circular economy approach, additional study is required to develop a mature technology. Furthermore, according to most literature on boron recovery/removal to obtain the necessary boron concentration for drinking water, the procedure aims to remove boron from the RO permeate stream [18]. Several studies have examined the effects of boron on other industrial sectors, such as Yan et al. [27]. As boron is a major issue for the production of Li_2CO_3(s), XSC-800 has been suggested as a boron-particular resin to eliminate it from refined brine [28]. Furthermore, Amberlite IRA-743 resin was used to eliminate boron by using wastewater produced by geothermal power plants [29]. The objective was to minimize the boron concentration in the wastewater so that it could be discharged.

Chelating resins are a class of adsorbents that are commonly used to remove heavy metal ions from aqueous solutions. One of the heavy metal ions that can be effectively removed by chelating resins is boron [30]. Chelating resins work by binding to boron ions in solution through a process called chelation, which involves the formation of a complex between the boron ions and the functional groups on the resin [31]. This complex is then removed from the solution through a process called adsorption, where the resin physically adsorbs the boron ions onto its surface. CRB05 is a specific type of chelating resin that is known for its ability to effectively remove boron ions from aqueous solutions [32]. The resin is made up of a synthetic polymer matrix that is functionalized with a specific chelating agent, in this case, the resin is functionalized with iminodiacetic acid (IDA) group which helps in binding to the boron ions [33]. Overall, CRB05 is a cost-effective and efficient way to remove boron from aqueous solutions. It is known for its high selectivity and capacity towards boron ions.

This research views the boron present in produced water as a possibility to deliver boron to industrial sectors rather than a problem. It is important to note that this method presents a considerable barrier in recovering boron from produced water at low concentrations to concentration levels suitable for secondary use in industrial plants. This makes the ion exchange stage crucial because it preferentially concentrates boron at greater than usual quantities. As a result, even with the use of resins, the boron extraction method provided in this study presents a new situation. Therefore, this study seeks to establish the ideal situation for boron sorption and desorption utilizing the boron selective resins DIAION™ CRB05. This resin adsorbent has been selected for this research due to its high selectivity and capacity for boron ions, as well as its stability and ease of regeneration. Additionally, DIAION CRB05 is effective in a wide range of pH and temperature conditions, making it suitable for use in a variety of industrial and research settings. Overall, DIAION CRB05 has been selected as the adsorbent of choice for boron due to its superior performance and versatility compared to other available resins. Thus, the objectives that guided this research were to: (i) characterize the DIAION™ CRB05 (ii) optimize the treatment process by RSM, and (iii) determine the best isotherm, and kinetic models based on adsorbent performance.

2. Materials

2.1. Resins and Reagents

In this study, CRB05 from Mitsubishi Chemical was used. It consists of a crosslinked matrix of microporous polystyrene coupled to functional groups of N-methyl-D-glucamine (NMDG). Chelating resins with "vis-diols", or ligands having contiguous phenolic hydroxyl groups, and hydroxyl groups in the cis position, exhibit high boron selectivity and rarely react with other elements [34]. Complexation processes result in selective sorption. Hydroxyl groups produce different borate esters with boric acid, and the proton produced throughout this intercalation is caught by the tertiary amine group [35]. Synthetic boron

solutions were prepared with boric acid (H_3BO_3) ACS reagent, ≥99.5% while Hydrochloric acid (HCL) ACS reagent, 37% was used for desorption.

2.2. Preparation of Standard Solutions

The boron stock solution (30%) was synthesized from a reagent of high grade. Before conducting the adsorption investigations, appropriate solutions were carefully prepared by H_3BO_3 ACS reagent, ≥99.5% with distilled water.

2.3. Characterization Methods

The morphology of the adsorbent material has been analyzed by FESEM. The XRD pattern of the adsorbent sample was examined to analyze the peaks present in the adsorbent material. Further, the associated bond vibrations present on the surface were examined by FTIR.

2.4. Batch Adsorption Studies and Analytical Methods

During batch adsorption tests, different concentrations of adsorbents, and initial concentrations of boron were by utilizing a stock solution of 30%, the stock solution was prepared by using boric acid and distilled water was added to 500 mg/L volumetric flasks. By using diluted HCl and NaOH to adjust the pH of boron solutions and shaking at 140 rpm in an orbital shaker for a different time, the impact of pH was investigated. Once the predetermined period had passed (30, 255, and 480 min), a filter membrane was used to extract the adsorbent from the liquid.

2.5. Analytical Methods

Using a HACH DR-3900 Spectrophotometer and the carmine technique, residual boron was measured. All the tests were triplicate. The procedure listed below was started for the boron concentration analysis: 75 mL of sulfuric acid into a 100 mL conical flask, in a well-ventilated area, one bag of BoroVer^3 B reagent powder pillow was poured into the flask, and the flask was swirl for five minutes to fully liquefy the powder, 0.2 mL of distilled water was used to one of the 16 mm tubes and another 0.2 mL of sample-filtered boron. A total of 3.5 mL of the BoroVer^3 Solution was added to the prepared sample tube and blank, the tubes were inverted to mix the solution with samples. After a 30 min reaction time, the measurement was conducted.

2.6. Response Surface Optimization RSM

Science research utilized the response surface methodology (RSM), a technique for improving testing procedures and methods [36]. Similar to the central composite design, the Box–Behnken response surface optimization design of experiments is much more effective. Consequently, the Box–Behnken design was fitted for this study's optimization [37,38]. Four parameters (Adsorbents Dosage, Time, Initial concentration of B, and pH) were investigated to find the major influence and reaction of the compound adsorbent for the adsorption of boron, and the adsorption settings within the experimental range were optimized. Table 1 illustrates the connection between the four-level codes of the four components and the experiment values, while Table 2 highlights the proposed runs matrix and the response. The adsorbent dosage and time affect the efficiency of boron removal, while the initial concentration of boron and the pH of the solution can also play a role in influencing the boron removal, adjusting these parameters can influence boron removal.

Table 1. Factor ranges in the Box–Behnken research setup.

Parameter	Lower Limit	Upper Limit
pH	2	7
Boron initial concentration (mg/L)	300	2000
Contact time (min)	30	480
Adsorbent dose (mg/L)	250	2000

Table 2. Design of experiments matrix and the responses generated by Box–Behnken Design.

Run	Factor 1	Factor 2	Factor 3	Factor 4	Response
	A: pH	B: Concentration of Boron	C: Contact Time	D: Adso. Dosage	Boron Residual
		(mg/L)	(min.)	(mg/L)	(mg/L)
1	7	1150	30	1125	35
2	4.5	1150	255	1125	22
3	7	1150	255	250	38
4	4.5	1150	255	1125	22
5	4.5	1150	480	2000	15
6	4.5	2000	30	1125	35
7	4.5	2000	480	1125	18
8	4.5	1150	480	250	35
9	4.5	1150	30	250	40
10	7	300	255	1125	32
11	4.5	300	255	250	31
12	4.5	2000	255	250	37
13	2	1150	480	1125	20
14	2	300	255	1125	18
15	4.5	300	480	1125	22
16	4.5	1150	255	1125	25
17	2	1150	255	250	34
18	4.5	1150	30	2000	25
19	4.5	2000	255	2000	22
20	2	1150	30	1125	24
21	7	2000	255	1125	28
22	7	1150	480	1125	30
23	4.5	1150	255	1125	21
24	4.5	300	255	2000	20
25	7	1150	255	2000	27
26	4.5	1150	255	1125	25
27	2	1150	255	2000	15
28	2	2000	255	1125	20
29	4.5	300	30	1125	20

The adsorption capacity was the model's reaction (Y). The coded factor is obtained by the connection of independent parameters:

$$\begin{aligned}\text{Boron Residual} = {} & +23.00 + 4.92 \times A + 1.42 \times B - 3.25 \times C - 7.58 \times D - 1.50 \times \\ & AB - 0.2500 \times AC + 2.00 \times AD - 4.75 \times BC - 1.0000 \times BD - 1.25 \times CD + 1.92 \times \\ & A^2 - 0.3333 \times B^2 + 1.67 \times C^2 + 4.17 \times D^2\end{aligned} \quad (1)$$

The equation demonstrated in light of the coded factors can be applied to foresee the outcome of different levels for every factor. High values of the elements are recorded as +1, while the low levels are coded as −1. The coded equation helps determine the relative importance of the elements by evaluating the factor coefficients.

2.7. Kinetic Modeling

Applying four distinct kinetic models; pseudo-first order, pseudo-second order, elovich, and intraparticle diffusion—the reaction rate and linked kinetic variables of boron sorption on CRB05 were investigated. In this research, the given Equations (1)–(4) forms of kinetic models were assumed [39–41].

$$\log(q_e - q_t) = \log q_e - \left(\frac{k1}{2.303}\right)t \qquad \text{pseudo first order model} \tag{2}$$

$$\left(\frac{t}{q_t}\right) = \left(\frac{1}{k2q_e2}\right) + \left(\frac{1}{q_e}\right)t \qquad \text{pseudo} - \text{second} - \text{order model} \tag{3}$$

$$q_t = \left(\frac{1}{b}\right)\ln(ab) + \left(\frac{1}{b}\right)\ln t \qquad \text{elovich model} \tag{4}$$

$$q_t = \left(kit\frac{1}{2}\right) + C_i \qquad \text{intraparticle} - \text{diffusion model} \tag{5}$$

2.8. Isotherm Models

An adsorption is a group of mass transfer processes that, in general, refers to the adherence of a sample to the surface of a liquid or solid (adsorbent). Adsorption isotherms describe the relationships between adsorbent and adsorbate at a known temperature in equilibrium. Many isotherm models may accurately match experimental data to identify a suitable model for the design process. The variables derived from different models give crucial information regarding the mechanism, surface features, and sorbent affinities [42]. During this research, the experimental data was validated using isotherm models to determine their applicability. Langmuir, Freundlich, and Temkin's isotherm models were all used in consideration of the boron sorption data at different initial concentrations. Isotherm analysis was carried out with linear formulas [43,44]. In this section, isotherm models obtained by adapting test findings to Freundlich, Langmuir, and Temkin are provided in Equations (5)–(7), respectively. The *Qm* was estimated using Langmuir's isotherm model. It provides a complete monolayer exposure on the surface of the sorbent. The linear formulation of Langmuir's isotherm is as follows:

$$\left(\frac{C_e}{q_e}\right) = \left(\frac{C_e}{q_L}\right) + \left(\frac{1}{q_L k_L}\right) \qquad \text{Langmuir model} \tag{6}$$

As a result, the unknown coefficients will be discovered by plotting *Ce*/*qe* against *Ce*. Freundlich's isotherm is an experimental formula for describing heterogeneous systems, and it is written as follows:

$$\ln(q_e) = \ln\left(K_f\right) + \left(\frac{1}{n_f}\right) + \ln C_e \qquad \text{Freundlich model} \tag{7}$$

K_f relates to the amount of boron absorbed on the adsorbent and is related to bonding energy. The n_f number indicates the amount of nonlinearity in the relationship between boron concentration and adsorption [45].

Temkin's isotherm equation includes an adsorption interaction factor, which is known as the heat of adsorption [46]. Temkin's equation is as follows:

$$Q_e = BtlnA_t + BtlnC_e \qquad \text{Temkin}'\text{s isotherm} \tag{8}$$

3. Results and Discussions

3.1. Characterization

For the characterization of raw CRB05 and after loading, various characterization methods were investigated, and the results are presented in this part as follows.

3.1.1. XRD

Essentially, the same XRD pattern was obtained before and after the Boron experiments for CRB05. Figure 1. depicts that there was no significant difference between before and after Boron experiments on CRB05; no peak was identified that was associated with compounds that contained boron. The ion exchange of borate ions with sulphate ions in

ettringite should be attributed to the removal of boron, and ettringite might be transferred to charlesite, a crystalline mineral with an ettringite-like structure in which boric ions were integrated rather than sulphate ions. The present case was not observed to exhibit a peak attributed to charlesite since raw ettringite content was small and the range of ion exchange was small [47–49]. The other low-intensity peak of CRB05 appeared at 70°. ZH Dastgerdi et al. analyzed the XRD pattern of adsorbent, they emphasized two peaks which are at 2θ = 24.9, 42.1° [50]. The peaks of CRB05 at 17.5° and 23.4° also proved to be acidic. When the other XRD spectrum is examined, a sharp peak of pure CRB05 is seen at 18.5° [51]. Venkatesan et al. defined the characteristic peak of adsorbent at 2θ = 20° [52]. The peak at 2θ ≈ 20.40° represents the functionalized-CRB05 material which is a highly used material. There was no significant change in XRD in this study, this suggests that the crystal structure of the material does not change significantly with the contact time, indicating that it is relatively stable under the conditions tested. It is possible that the sample is being exposed to some kind of environmental condition (e.g., contact time, adsorbent dosage, initial concentration and pH), and the results are being used to understand the stability of the material under those conditions [53].

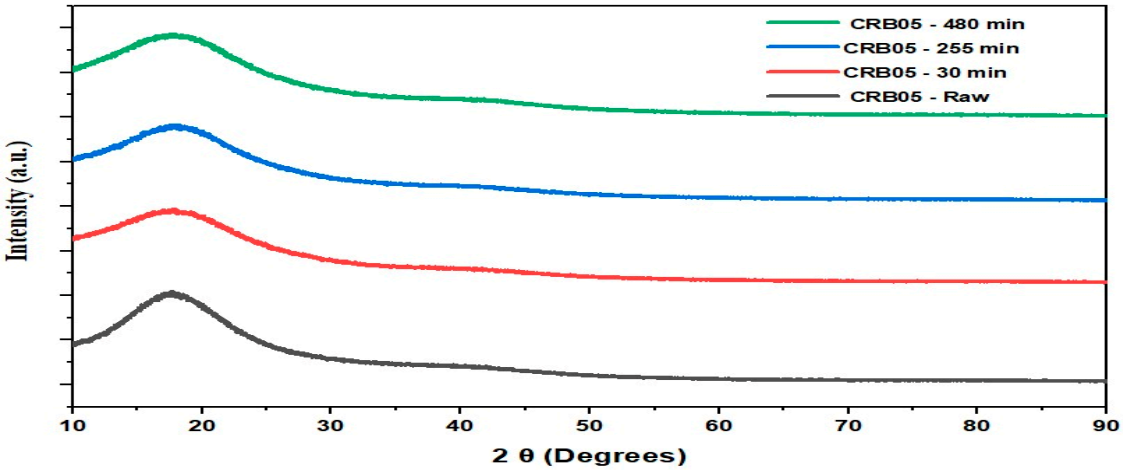

Figure 1. XRD patterns for CRB05 before and after boron removal experiments.

3.1.2. FTIR

FTIR spectra of raw, 30 m, 255 m, and 480 m are shown in Figure 2. Broad peaks were seen for CRB05 before and after the removal of the boron, at 30 m, 255 m, and 480 m at 3450–3000 cm^{-1}, that have been linked to the O–H stretching vibration [54]. The H–O–H was in charge of the peak near 1500 cm^{-1}. At 1652 cm^{-1}, the other O–H group showed up [55]. Another stretching peak was found near 1630–1653 cm^{-1} and was attributed to the N-acetyl group because of amide 1 stretching. The existence of two comparatively small peaks at 1500–1100 cm^{-1} and close 1122 cm^{-1}, that have been appointed to B–O and B–O–H bonds, respectively, confirmed B sorption [56]. Similar peaks were observed, this may be due to the presence of the adsorbent molecules in the pores [57]. The miner change in FTIR, suggests that the chemical composition of the material is slightly affected by the parameters such as initial concentration, adsorbent dosage, pH, and contact time [58]. This could mean that the material is relatively stable under the conditions tested, but it is also possible that the change is due to the presence of impurities or small amounts of a different compound that are not present in the raw sample. It is also possible that the functional groups present in the sample have been slightly modified by the parameter that has been used [59].

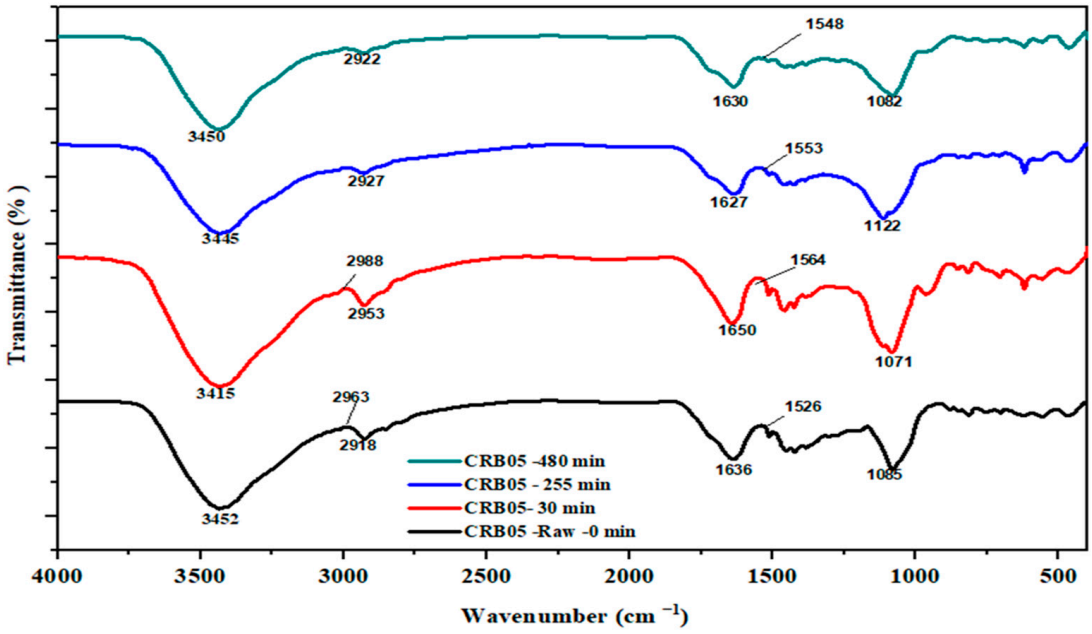

Figure 2. FTIR peaks for CRB05 before and after boron removal experiments.

3.1.3. FESEM

Figure 3a,b show the surface morphologies and elemental compositions of the CRB05 before and after adsorption. The FESEM image showed that the uniform spherical particles were agglomerated. Before and after adsorption, the morphology of the two samples changes. CRB05, on the other hand, showed up to have a regular hexagonal structure with an estimated size of 2–5 m and a thickness of 500 nm. The pores shaped were invariably scattered across the entire surface of the materials, giving active adsorption sites [60,61]. A comparison of the surface morphology before and following adsorption demonstrates that boron is being taken up over the surface of CRB05, as the bores appear to be filled up.

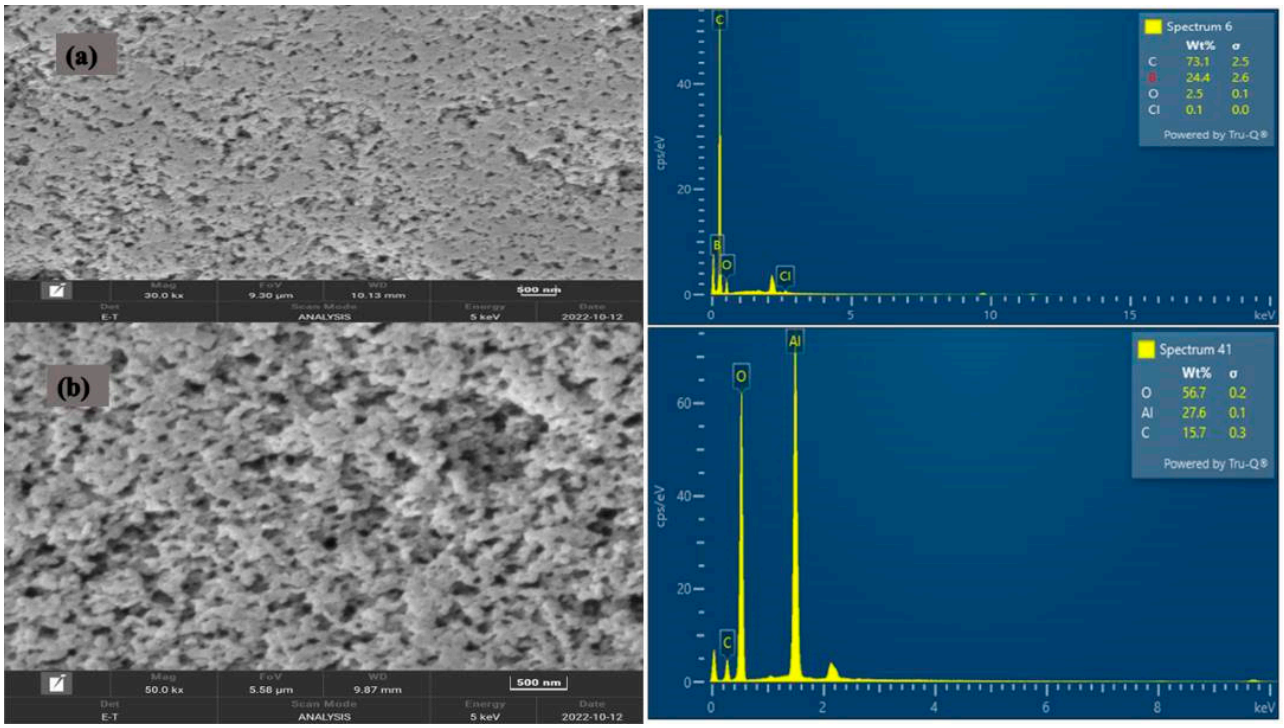

Figure 3. FESEM and EDX of (**a**) Before loading CRB05 (**b**) After loading CRB05.

3.2. Optimizing Procedure

3.2.1. Representation of a Regression Model

Surface response methodology (RSM) is used to analyze how various input parameters correlate with output responses. The Box-Cox plot in this research recommends log transformation of power (see Figure 4). The green line illustrates the ideal value of λ, while the blue line shows the current value. The blue line was inserted between the two red lines by adding a Log transformation [62].

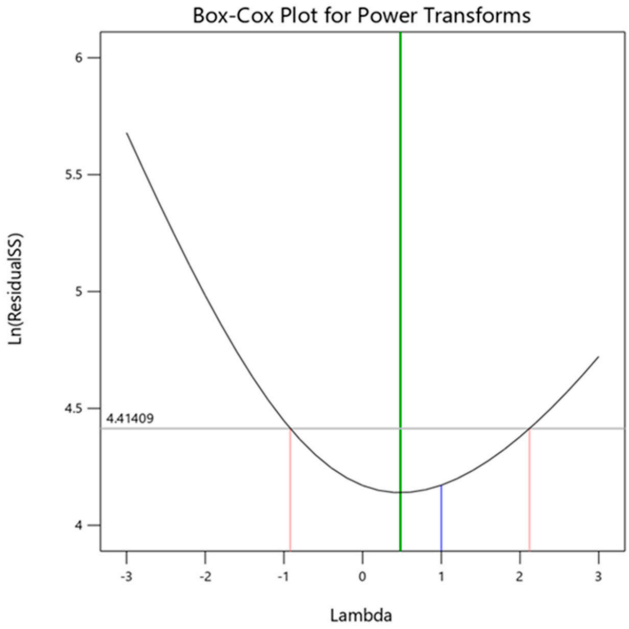

Figure 4. Transformation of model power.

3.2.2. Statistical Analysis of Variance (ANOVA)

There were four main regression models designated: linear, 2FI, cubic, and quadratic. CRB05 recommended the quadratic model as the perfect match for boron removal. In Table 3, the value corresponds to the highest R^2 of 0.9556. The Predicted R^2 of 0.7844 supports the Adjusted R^2 of 0. 9112; the variation should be less than 0.2. The signal-to-noise ratio is found by Adeq Precision. A ratio bigger than four is preferred. The signal-to-noise ratio of 16.1532 showed a good signal. Using this model will help move around the design space.

Table 3. Values of Regression Analysis.

Std. Dev.	2.15	R^2	0.9556
Mean	26.07	Adj R^2	0.9112
C.V. %	8.25	Pred R^2	0.7844
		Adeq Precision	16.1532

The model's F-value of 21.52 shows the model is significant. An F-value such as big might happen because of noise just 0.01% of the time. In this model, it was found that the (A, B, C, D, BC, A2, D2) are all significant model terms in this case as *p*-values less than 0.0500. The Lack of Fit F-value of 1.45 highlighted in Table 4 shows that the Lack of Fit is insignificant in comparison to the pure error. A non-significant lack of fit is desirable because the design is required to be accurate.

The coefficient R^2 in Table 3 is (0.9556), implying this model explained 95% of the variation [63]. The model is well predictable because of the difference between Adj. R^2

and Pre. R^2 is less than 0.2. The standard deviation in this model is 2.15. The lower the standard deviation, the nearer the predicted value is to the actual response value. The coefficient, which evaluates the precision and dependability of the experiments, is 8.25%. More precision and more logical experiments are implied by a smaller value of the coefficient of different C.V. The exact values are derived from runs of tests that have been conducted, and the Pred values come from the model applying the Pred equation in design expert software. Figure 5 illustrates the actual values versus the Pred values of the response of surface area. A favorable connection between the actual and predicted points of the response can be seen from the values' proximity to the straight line. Since the suggested quadratic model is sufficiently equipped to indicate the reaction of variables and response, statistical tests support this conclusion.

Table 4. ANOVA of Quadratic Model of CRB05 with the response of surface area.

Source	Sum of Squares	df	Mean Square	F-Value	*p*-Value	
Model	1395.03	14	99.64	21.52	<0.0001	significant
A-pH	290.08	1	290.08	62.64	<0.0001	
B-Conc. of Boron	24.08	1	24.08	5.20	0.0388	
C-Contact time	126.75	1	126.75	27.37	0.0001	
D-Adso Dosage	690.08	1	690.08	149.02	<0.0001	
AB	9.00	1	9.00	1.94	0.1850	
AC	0.2500	1	0.2500	0.0540	0.8196	
AD	16.00	1	16.00	3.46	0.0842	
BC	90.25	1	90.25	19.49	0.0006	
BD	4.00	1	4.00	0.8638	0.3684	
CD	6.25	1	6.25	1.35	0.2648	
A^2	23.83	1	23.83	5.15	0.0397	
B^2	0.7207	1	0.7207	0.1556	0.6992	
C^2	18.02	1	18.02	3.89	0.0686	
D^2	112.61	1	112.61	24.32	0.0002	
Residual	64.83	14	4.63			
Lack of Fit	50.83	10	5.08	1.45	0.3838	not significant
Pure Error	14.00	4	3.50			
Cor Total	1459.86	28				

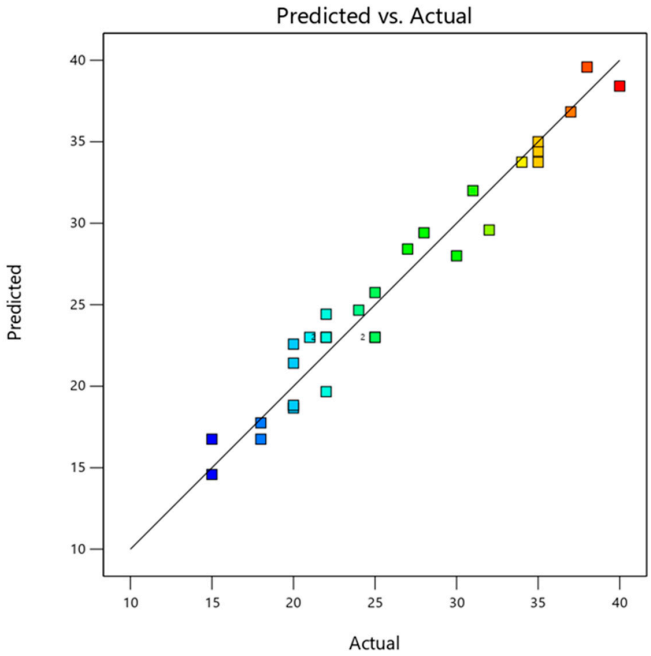

Figure 5. Predicted response vs. actual response for surface area.

3.2.3. The Influence of a Factor's Correlation on a Response

A 3D response surface plot can illustrate intuitively how many different affecting factors (Adsorbent Dosage, pH, Time, and initial Concentration of Boron) have an impact on response value (boron adsorption capacity). The 3D response surface plots in Figure 6a–f provide a clear representation of the impact that various influential factors Adsorbent Dosage, pH, Time, and initial Concentration of Boron) have on the response value (boron adsorption capacity). The rate of adsorption impact began to stabilize, rather than continue to increase, suggesting that the potential benefits of the adsorbent are limited. This concept could be caused by an increase in adsorbent dosage, which also strengthens the gradient of boron outside the adsorbent and impedes boron accumulation and diffusion on the adsorbent [64,65]. Figure 6a illustrates the interaction between initial concentration to pH. More boron is removed at lower pH levels. Boron removal typically increases at lower pH values because at lower pH, boric acid (H_3BO_3) is the dominant form of boron present, and it is more easily adsorbed by adsorbents such as aluminum hydroxide and iron hydroxide [66]. As the pH increases, other forms of boron such as borates (BO_3 and BO_4) become more prevalent, which are less readily adsorbed by these adsorbents. Additionally, the acidity of the water can affect the surface charge of the adsorbent, making it more attractive to the positively charged boric acid molecules [67]. Figure 6b, and d illustrated the interaction of pH to adsorbent dosage and contact time. The high point at acidic pH 2 is located at 255 min. Figure 6c illustrated the interaction between Adsorbent Dose and pH. It is evident that when the adsorbent dosage is 2000 mg/L and pH = 2, the surface impact of adsorbent dosage and pH is almost at its peak. Figure 6e shows the interaction between the adsorbent Dose and initial boron concentration. The adsorption efficiency has increased as a result of the addition of these two factors. In comparison, the impact of contact time on adsorption performance is noticeably greater than the impact of adsorbent dosage [68]. Additionally, response surface analysis in the research category predicts the ideal adsorption conditions for boron in addition to CRB05: adsorbent dosage = 1782 mg/L, pH = 2.8, initial concentration, 1617 mg/L, and time = 475 min. The highest boron adsorption capacity that may be predicted under these circumstances is 12.11 mg/L. Adsorption tests have been performed to establish the accuracy of effective adsorption, and the observed value was 11.6 mg/L. The response surface model predicted the best experimental conditions. The model's prediction is practical and efficient; moreover, the possibility of using the models to predict and enhance the adsorption of boron by CRB05 because the difference between the predicted value and experimental values is small.

The change in the initial pH of the solution medium in the adsorption process is very important for the functioning of the adsorption process. Since the pH change leads to protonation or deprotonation on the adsorbent surface, the optimum pH value must be determined for the adsorption to occur favorably [69]. Boron adsorption on CRB05 occurs through positive or negative groups on the surface. Within the scope of this study, the pH change and its effect were studied in the pH range of 2–7 and the optimum pH value was determined as approximately two for further studies. The plot showing the pH change is given in Figure 6a–c. It is seen that the adsorption capacity reaches maximum levels at pH values between 2 and 4.5 but is lower at other pH values. At the pH where the adsorbent surface is neutral, the adsorption reaches its maximum value.

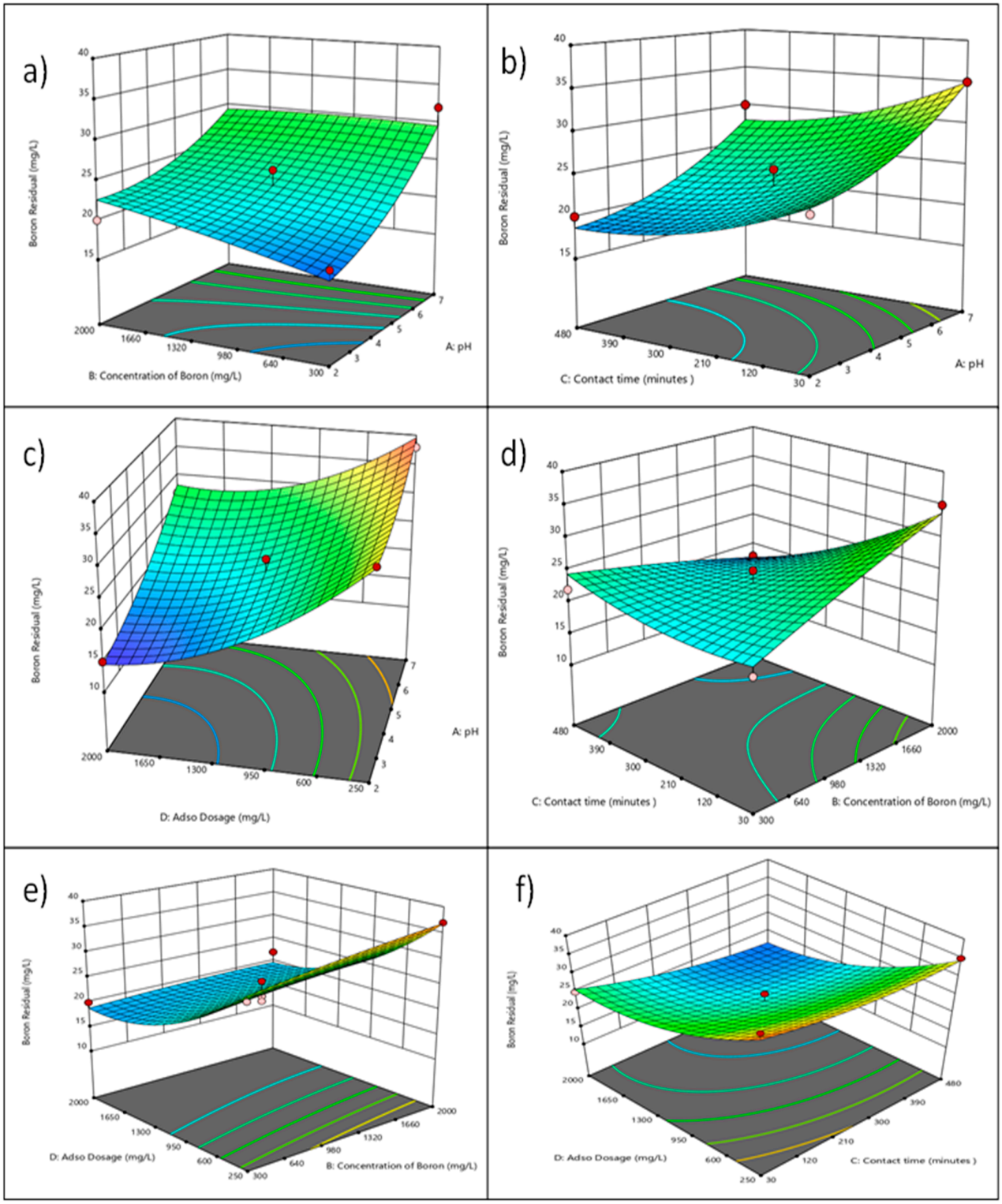

Figure 6. Interaction of (**a**) Initial Concentration and pH (3D surface); (**b**) Time and pH (3D surface); (**c**) Adsorbent Dosage and pH (3D surface); (**d**) Time and Initial concentration (3D surface); (**e**) Adsorbent Dose and Initial Concentration (3D surface); (**f**) Adsorbent Dosage and Time (3D surface).

3.3. Kinetic Studies

Adsorption kinetic research is required to examine the reaction's principle and learn about the best adsorption operating conditions. As a result, certain kinetic models for B adsorption have been used. The linear forms for the pseudo-first-order, pseudo-second-

order, intraparticle-diffusion model, and Elovich kinetic models have been employed to assess the boron kinetics. The kinetic graphs shown in Figure 7a–f confirmed that the value of q_e derived by the pseudo-first-order reaction equation was nearer to the q_e determined by tests. The calculation of kinetic parameters is presented in Table 5 and linearizing a model can change the error distribution of experimental data. For example, the term t/q_t in the pseudo-second-order linear form is not defined at $t = 0$, but linearization will make the error distribution Gaussian, resulting in new parameter values. Additionally, in the linear form, the term $\ln(q_e - q_t)$ becomes undefined at equilibrium ($q_e = q_t$) [70]. The kinetics of the procedure was therefore likely pseudo-first-order. This conclusion was supported by the kinetic model's R^2 value, which was close to unity. The adsorption mechanism could be influenced by both boron and the amount of adsorbent, based on a typical pseudo-first-order reaction [71]. Elovich's kinetic model is another kinetic equation that was used to assess boron adsorption. The plot of this Elovich's kinetic is shown in Figure 7. Chemical adsorption mechanisms are responsible for Elovich's kinetic model, which is why this equation's R^2 value was low compared to another kinetic model. It indicated that the mechanism for adsorption may be getting closer to physical adsorption. The intraparticle diffusion kinetic model for boron adsorption by CRB05 is a specific model that describes the adsorption of boron ions onto a specific adsorbent material, CRB05 [72]. It typically includes equations that describe the rate of diffusion of boron ions through the CRB05 particles and the rate of chemical reactions that occur between the boron ions and the CRB05 surface [32]. The model can be used to predict the number of boron ions that will be adsorbed onto the CRB05 over time, as well as the rate at which the adsorption will occur. The intraparticle diffusion kinetic model was evaluated to investigate the rate-finding stage at which boron adsorption by CRB05 [73]. This equation's plot confirmed linear zones, demonstrating how multiple processes had an impact on the adsorption by the adsorbent. The R^2 value was 0.9968, demonstrating the usefulness of this model, and this might support the hypothesis that the rate-limiting step was intraparticle diffusion [74]. Additionally, the results of this model can be used to predict the adsorption behavior of the system under different conditions and to optimize the adsorption process. The calculation of kinetic parameters is presented in Table 5 and linearizing a model can change the error distribution of experimental data. For example, the term t qt in the pseudo-second-order linear form is not defined at $t = 0$, but linearization will make the error distribution Gaussian, resulting in new parameter values. Comparing the pseudo-first-order model, two different approaches yielded significantly different parameter values. Additionally, in the linear form, the term $\ln(q_e - q_t)$ becomes undefined at equilibrium ($q_e = q_t$).

Table 5. Comparison of the kinetics parameters.

Kinetic Model	Parameter	
Pseudo-First Order Model	Q_e	1.289
	K_1	0.0006
	R^2	0.997
Pseudo Second Order Model	q_e	4
	k_2	0.129
	R^2	0.975
intraparticle − diffusion model	k_{dif}	0.456
	C	15.3
	R^2	0.996
Elovich kinetic Model	B	875
	A	65.66
	R^2	0.910

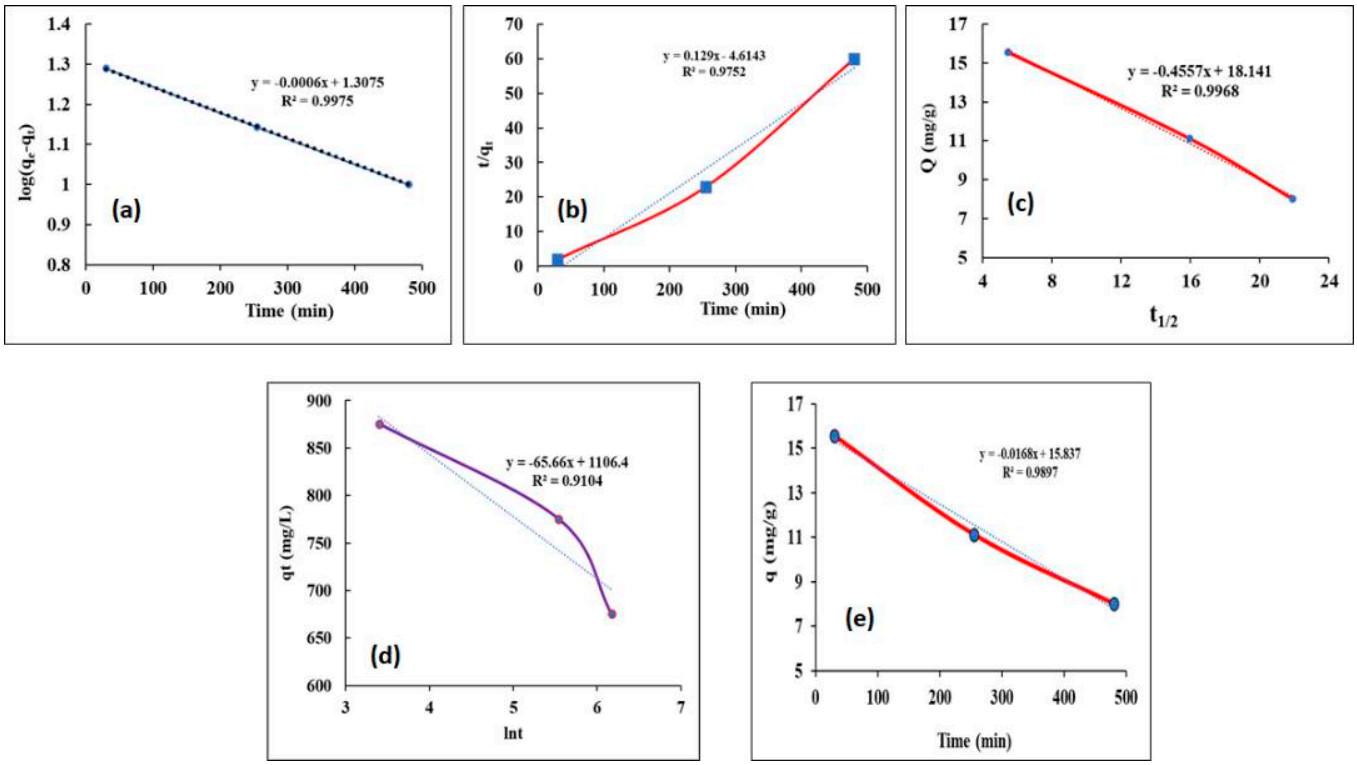

Figure 7. Adsorption kinetics fitted with (**a**) Pseudo-First-Order, (**b**) Pseudo-Second-Order (**c**) Intra-particle Diffusion Kinetics Models, and (**d**) Elovich Kinetic Model (**e**) Effect of adsorption time on the boron adsorption.

3.4. Isotherm

Adsorption is a technique that transfers mass processes that, in principle, refers to the adherence of a sample to the surface of a liquid or solid (adsorbent). Adsorption isotherms are terms for relationships between the adsorbent and adsorbate at a known time in equilibrium. To select the most relevant model for the design process, experimental data can be used to successfully fit several isotherm models. The parameters derived from various models offer crucial data regarding the mechanism, surface features, and sorbent affinities [75]. Throughout this study, the data collected was validated using isotherm models to determine their applicability. These isotherm models compute the values of the coefficients. The Q_m was estimated using Langmuir's isotherm model. It signifies a complete surface monolayer exposure of the sorbent; therefore, the unidentified coefficients will be discovered by creating a plot of C_e/q_e against C_e (see Figure 8). The coefficients calculated by the isotherm models were recorded in Table 6. Langmuir's isotherm model, which was used to estimate Q_m and assumes a monolayer coverage of the sorbent surface. The linear form of Langmuir's isotherm can be written as follows:

$$\left(\frac{C_e}{q_e}\right) = \left(\frac{1}{K_a Q_m}\right) + \left(\frac{1}{Q_m}\right) C_e \tag{9}$$

Freundlich's isotherm is a mathematical equation that describes heterogeneous structures in experimental data, and it can be represented as follows [76]:

$$\ln(q_e) = \ln\left(K_f\right) + \left(\frac{1}{n_f}\right) + \ln C_e \tag{10}$$

The K_f value is linked to the bonding energy and indicates the amount of dye adsorbed on the adsorbent. The n_f value is used to gauge the nonlinearity of the relationship between dye concentration and adsorption. If n_f is equal to 1, it indicates linear adsorption, if n_f is less

than one, it suggests a chemical adsorption process and if n_f is greater than one, it suggests physical adsorption. Based on Table 6, the value of n_f for Boron adsorption by CRB05 is greater than one, suggesting that the adsorption process is physical. The findings and R^2 value confirmed that the equilibrium of adsorption given by Freundlich's isotherm was preferable to Langmuir's isotherm. Because of this, it is possible that CRB05 adsorption took place on the varied surface of boron while the molecules that were adsorbed were engaging. The high correlation coefficients R^2 = 0.9908 of the aforementioned models demonstrated the accuracy match up of the adsorption experimental results to these two models. Temkin's isotherm equation includes an adsorption interaction factor, which is known as the heat of adsorption [77]. The linear isotherm constants and coefficients were determined by plotting q_e versus Ln(C_e), as shown in Figure 8c. Temkin's isotherm was found to be the best fit for the boron adsorption onto CRB05, according to data analysis that revealed a high correlation coefficient. This isotherm models the adsorption process as being influenced by physical interactions between the adsorbent (CRB05) and the adsorbate (boron).

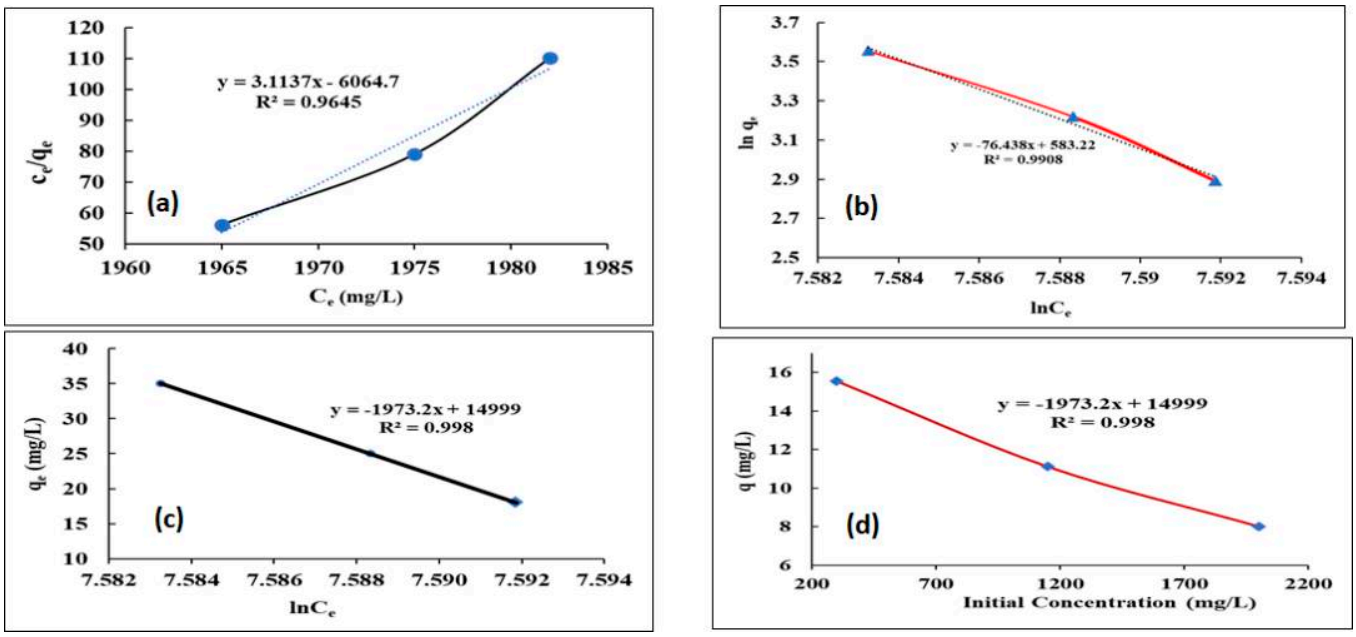

Figure 8. The adsorption isotherms of B fitted lines with the (**a**) Langmuir (**b**) Freundlich (**c**) Temkin (**d**) Effect of the initial concentration on the boron adsorption.

Table 6. Comparison of the isotherm's parameters.

Isotherm Model	Parameter	
Langmuir	Q_m (mg g^{-1})	55
	K_a (L mg^{-1})	3.1
	R^2	0.964
Freundlich	n_f	76.4
	K_f (L g^{-1})	3.5
	R^2	0.990
Temkin	A_T	34
	b_T	−1973.2
	R^2	0.998

4. Conclusions

The adsorptive removal of boron from aqueous solutions by DIAION™ CRB05 was effective. The adsorption process was optimized through response surface methodology. During the adsorption studies, 98% was the greatest adsorption rate attained. The dosage

was reported to be 2000 mg/L at pH 2 and boron's initial concentration of 1115 mg/L with 255 min for the highest removal anticipated from RSM. Characterized by various techniques, including XRD, FTIR, and FESM. The kinetics of the adsorption process was studied using different models, such as the Pseudo Second Order Model, Pseudo First Order Model, Intraparticle Diffusion Model, and Elovich Kinetic Model. Isotherm studies were also conducted using Langmuir, Freundlich, and Temkin models. It was discovered that the Temkin isotherm and the pseudo-first-order model were found to have good fits after comparison with R^2 (0.998, and 0.9975), respectively. According to the activation energy value derived using the First-order rate constants generated from this kinetic model, it might be demonstrated that the adsorption occurs physically, due to thermodynamic research. The results indicate that DIAION™ CRB05 is an effective adsorbent for removing boron from aqueous solutions.

Author Contributions: Conceptualization, B.N.S.A.-d. and S.R.M.K.; methodology, S.R.M.K., B.N.S.A.-d. and G.H.; supervision, S.R.M.K.; project administration, S.R.M.K. and G.H.; funding acquisition, S.R.M.K., B.M.E.E., A.H.J. and M.M.; software, B.M.E.E., A.N. and M.M.; validation, G.H., A.A.H.S., N.M.Y.A.-M. and A.A.-N.; formal analysis, B.N.S.A.-d., A.H.J., N.M.Y.A.-M. and A.A.-N.; resources, S.R.M.K. and A.H.J.; data curation, A.A.H.S., A.N. and M.M.; writing—original draft preparation, B.N.S.A.-d.; writing—review and editing, B.N.S.A.-d., S.R.M.K., G.H. and A.H.J.; visualization, A.N., B.M.E.E. and A.A.H.S. All authors have read and agreed to the published version of the manuscript.

Funding: This research was funded by Universiti Teknologi PETRONAS (UTP) under YUTP grant cost center 015LC0-361. This Study is supported via funding from Prince Sattam bin Abdulaziz University project number (PSAU/2023/R/1444).

Data Availability Statement: The data presented in this study are available from the corresponding authors upon reasonable request.

Acknowledgments: The authors would like to offer their deep gratitude to UTP and (YUTP) under grant cost center 015LC0-361. This study is supported via funding from Prince Sattam bin Abdulaziz University project number (PSAU/2023/R/1444).

Conflicts of Interest: The authors declare no conflict of interest.

References

1. Eljamal, O.; Maamoun, I.; Alkhudhayri, S.; Eljamal, R.; Falyouna, O.; Tanaka, K.; Kozai, N.; Sugihara, Y. Insights into boron removal from water using Mg-Al-LDH: Reaction parameters optimization & 3D-RSM modeling. *J. Water Process. Eng.* **2022**, *46*, 102608. [CrossRef]
2. Birniwa, A.H.; Mohammad, R.E.A.; Ali, M.; Rehman, M.F.; Abdullahi, S.S.A.; Eldin, S.M.; Mamman, S.; Sadiq, A.C.; Jagaba, A.H. Synthesis of Gum Arabic Magnetic Nanoparticles for Adsorptive Removal of Ciprofloxacin: Equilibrium, Kinetic, Thermodynamics Studies, and Optimization by Response Surface Methodology. *Separations* **2022**, *9*, 322. [CrossRef]
3. Kanoun, O.; Lazarević-Pašti, T.; Pašti, I.; Nasraoui, S.; Talbi, M.; Brahem, A.; Adiraju, A.; Sheremet, E.; Rodriguez, R.; Ben Ali, M.; et al. A Review of Nanocomposite-Modified Electrochemical Sensors for Water Quality Monitoring. *Sensors* **2021**, *21*, 4131. [CrossRef] [PubMed]
4. Al-dhawi, B.N.S.; Kutty, S.R.M.; Ghaleb, A.A.S.; Almahbashi, N.M.Y.; Saeed, A.A.H.; Al-Mekhlafi, A.B.A.; Alsaeedi, Y.A.A.; Jagaba, A.H. Pretreated palm oil clinker as an attached growth media for organic matter removal from synthetic domestic wastewater in a sequencing batch reactor. *Case Stud. Chem. Environ. Eng.* **2022**, *7*, 100294. [CrossRef]
5. Melliti, A.; Kheriji, J.; Bessaies, H.; Hamrouni, B. Boron removal from water by adsorption onto activated carbon prepared from palm bark: Kinetic, isotherms, optimisation and breakthrough curves modelling. *Water Sci. Technol.* **2020**, *81*, 321–332. [CrossRef]
6. Usman, A.; Aris, A.; Labaran, B.; Darwish, M.; Jagaba, A. Effect of Calcination Temperature on the Morphology, Crystallinity, and Photocatalytic Activity of ZnO/TiO2 in Selenite Photoreduction from Aqueous Phase. *J. New Mater. Electrochem. Syst.* **2022**, *25*, 251–258. [CrossRef]
7. Birniwa, A.H.; Abdullahi, S.S.; Yakasai, M.Y.; Ismaila, A. Studies on physico-mechanical behaviour of kenaf/glass fiber reinforced epoxy hybrid composites. *Bull. Chem. Soc. Ethiop.* **2021**, *35*, 171–184. [CrossRef]
8. Wimmer, M.A.; Abreu, I.; Bell, R.W.; Bienert, M.D.; Brown, P.H.; Dell, B.; Fujiwara, T.; Goldbach, H.E.; Lehto, T.; Mock, H.; et al. Boron: An essential element for vascular plants. *New Phytol.* **2019**, *226*, 1232–1237. [CrossRef]
9. Jagaba, A.H.; Kutty, S.R.M.; Baloo, L.; Noor, A.; Abubakar, S.; Lawal, I.M.; Umaru, I.; Usman, A.K.; Kumar, V.; Birniwa, A.H. Effect of Hydraulic Retention Time on the Treatment of Pulp and Paper Industry Wastewater by Extended Aeration Activated Sludge System. In Proceedings of the 2021 Third International Sustainability and Resilience Conference: Climate Change (IEEE 2021), Sakheer, Bahrain, 15–16 November 2021; pp. 221–224.

10. Al-dhawi, B.; Kutty, S.R.; Almahbashi, N.; Noor, A.; Jagaba, A.H. Organics removal from domestic wastewater utilizing palm oil clinker (POC) media in a submerged attached growth system. *Int. J. Civ. Eng. Technol.* **2020**, *11*, 1–7.
11. Tomaszewska, B.; Bodzek, M.J.D. Desalination of geothermal waters using a hybrid UF-RO process—Part I: Boron removal in pilot-scale tests. *Desalination* **2013**, *319*, 99–106. [CrossRef]
12. Yaro, N.S.A.; Sutanto, M.H.; Habib, N.Z.; Napiah, M.; Usman, A.; Al-Sabaeei, A.M.; Rafiq, W. Feasibility Evaluation of Waste Palm Oil Clinker Powder as a Fillers Substitute for Eco-Friendly Hot Mix Asphalt Pavement. *Int. J. Pavement Res. Technol.* **2022**, 1–14. [CrossRef]
13. Jagaba, A.H.; Kutty, S.R.M.; Baloo, L.; Birniwa, A.H.; Lawal, I.M.; Aliyu, M.K.; Yaro, N.S.A.; Usman, A.K. Combined treatment of domestic and pulp and paper industry wastewater in a rice straw embedded activated sludge bioreactor to achieve sustainable development goals. *Case Stud. Chem. Environ. Eng.* **2022**, *6*, 100261. [CrossRef]
14. Ipekçi, D.; Altıok, E.; Bunani, S.; Yoshizuka, K.; Nishihama, S.; Arda, M.; Kabay, N. Effect of acid-base solutions used in acid-base compartments for simultaneous recovery of lithium and boron from aqueous solution using bipolar membrane electrodialysis (BMED). *Desalination* **2018**, *448*, 69–75. [CrossRef]
15. Sayed, K.; Baloo, L.; Kutty, S.R.B.; Al Madhoun, W.; Kankia, M.U.; Jagaba, A.H.; Singa, P.K. Optimization of palm oil mill effluent final discharge as biostimulant for biodegradation of tapis light crude petroleum oil in seawater. *J. Sea Res.* **2022**, *188*, 102268. [CrossRef]
16. Yaro, N.S.A.; Napiah, M.; Sutanto, M.H.; Usman, A.; Mizwar, I.K.; Umar, A.M. Engineering Properties of Palm Oil Clinker Fine-Modified Asphaltic Concrete Mixtures. *J. Eng. Technol. Sci.* **2022**, *54*.
17. Bangari, R.S.; Yadav, V.K.; Singh, J.K.; Sinha, N. Fe_3O_4-Functionalized Boron Nitride Nanosheets as Novel Adsorbents for Removal of Arsenic(III) from Contaminated Water. *ACS Omega* **2020**, *5*, 10301–10314. [CrossRef]
18. Jagaba, A.; Kutty, S.; Hayder, G.; Baloo, L.; Noor, A.; Yaro, N.; Saeed, A.; Lawal, I.; Birniwa, A.; Usman, A. A Systematic Literature Review on Waste-to-Resource Potential of Palm Oil Clinker for Sustainable Engineering and Environmental Applications. *Materials* **2021**, *14*, 4456. [CrossRef]
19. Akhoondi, A.; Feleni, U.; Bethi, B.; Idris, A.O.; Hojjati-Najafabadi, A. Advances in metal-based vanadate compound photocatalysts: Synthesis, properties and applications. *Synth. Sinter.* **2021**, *1*, 151–168. [CrossRef]
20. Al-Sabaeei, A.M.; Al-Fakih, A.; Noura, S.; Yaghoubi, E.; Alaloul, W.; Al-Mansob, R.A.; Khan, M.I.; Yaro, N.S.A. Utilization of palm oil and its by-products in bio-asphalt and bio-concrete mixtures: A review. *Constr. Build. Mater.* **2022**, *337*, 127552. [CrossRef]
21. Kameda, T.; Yamamoto, Y.; Kumagai, S.; Yoshioka, T. Analysis of F−removal from aqueous solutions using MgO. *J. Water Process. Eng.* **2018**, *25*, 54–57. [CrossRef]
22. Jagaba, A.H.; Kutty, S.R.M.; Isa, M.H.; Ghaleb, A.A.S.; Lawal, I.M.; Usman, A.K.; Birniwa, A.H.; Noor, A.; Abubakar, S.; Umaru, I.; et al. Toxic Effects of Xenobiotic Compounds on the Microbial Community of Activated Sludge. *ChemBioEng Rev.* **2022**, *9*, 497–535. [CrossRef]
23. Abdullahi, S.S.; Musa, H.; Habibu, S.; Birniwa, A.H.; Mohammad, R.E.A. Comparative study and dyeing performance of as-synthesized azo heterocyclic monomeric, polymeric, and commercial disperse dyes. *Turk. J. Chem* **2022**, *46*, 1–12. [CrossRef]
24. Birniwa, A.H.; Abubakar, A.S.; Mahmud, H.N.M.E.; Kutty, S.R.M.; Jagaba, A.H.; Abdullahi, S.S.A.; Zango, Z.U. Application of Agricultural Wastes for Cationic Dyes Removal from Wastewater. In *Textile Wastewater Treatment*; Springer: Singapore, 2022; pp. 239–274.
25. Jagaba, A.H.; Kutty, S.R.M.; Isa, M.H.; Affam, A.C.; Aminu, N.; Abubakar, S.; Noor, A.; Lawal, I.M.; Umaru, I.; Hassan, I. Effect of environmental and operational parameters on sequential batch reactor systems in dye degradation. In *Dye Biodegradation, Mechanisms and Techniques*; Springer: Berlin/Heidelberg, Germany, 2022; pp. 193–225.
26. Yaro, N.S.A.; Sutanto, M.H.; Habib, N.Z.; Napiah, M.; Usman, A.; Al-Sabaeei, A.M.; Rafiq, W. Mixture Design-Based Performance Optimization via Response Surface Methodology and Moisture Durability Study for Palm Oil Clinker Fine Modified Bitumen Asphalt Mixtures. *Int. J. Pavement Res. Technol.* **2022**, 1–28. [CrossRef]
27. Yan, S.C.; Li, Z.S.; Zou, Z.G. Photodegradation of Rhodamine B and Methyl Orange over Boron-Doped g-C_3N_4 under Visible Light Irradiation. *Langmuir* **2010**, *26*, 3894–3901. [CrossRef]
28. Jagaba, A.; Kutty, S.; Lawal, I.; Abubakar, S.; Hassan, I.; Zubairu, I.; Umaru, I.; Abdurrasheed, A.; Adam, A.; Ghaleb, A.; et al. Sequencing batch reactor technology for landfill leachate treatment: A state-of-the-art review. *J. Environ. Manag.* **2021**, *282*, 111946. [CrossRef]
29. Abdullahi, S.S.; Musa, H.; Habibu, S.; Birniwa, A.H.; Mohammad, R.E.A. Facile synthesis and dyeing performance of some disperse monomeric and polymeric dyes on nylon and polyester fabrics. *Bull. Chem. Soc. Ethiop.* **2022**, *35*, 485–497. [CrossRef]
30. Usman, A.; Sutanto, M.H.; Napiah, M.; Zoorob, S.E.; Yaro, N.S.A.; Khan, M.I. Comparison of performance properties and prediction of regular and gamma-irradiated granular waste polyethylene terephthalate modified asphalt mixtures. *Polymers* **2021**, *13*, 2610. [CrossRef]
31. Kankia, M.U.; Baloo, L.; Danlami, N.; Samahani, W.N.; Mohammed, B.S.; Haruna, S.; Jagaba, A.H.; Abubakar, M.; Ishak, E.A.; Sayed, K. Optimization of Cement-Based Mortar Containing Oily Sludge Ash by Response Surface Methodology. *Materials* **2021**, *14*, 6308. [CrossRef]
32. Birniwa, A.H.; Mahmud, H.N.M.E.; Abdullahi, S.S.; Habibu, S.; Jagaba, A.H.; Ibrahim, M.N.M.; Ahmad, A.; Alshammari, M.B.; Parveen, T.; Umar, K. Adsorption Behavior of Methylene Blue Cationic Dye in Aqueous Solution Using Polypyrrole-Polyethylenimine Nano-Adsorbent. *Polymers* **2022**, *14*, 3362. [CrossRef]

33. Yaro, N.S.A.; Sutanto, M.H.; Habib, N.Z.; Napiah, M.; Usman, A.; Jagaba, A.H.; Al-Sabaeei, A.M. Application and circular economy prospects of palm oil waste for eco-friendly asphalt pavement industry: A review. *J. Road Eng.* **2022**, *2*, 309–331. [CrossRef]
34. Jagaba, A.H.; Kutty, S.R.M.; Lawal, I.M.; Birniwa, A.H.; Affam, A.C.; Yaro, N.S.A.; Usman, A.K.; Umaru, I.; Abubakar, S.; Noor, A. Circular economy potential and contributions of petroleum industry sludge utilization to environmental sustainability through engineered processes—A review. *Clean. Circ. Bioecon.* **2022**, *3*, 100029. [CrossRef]
35. Gazi, M.; Shahmohammadi, S. Removal of trace boron from aqueous solution using iminobis-(propylene glycol) modified chitosan beads. *React. Funct. Polym.* **2012**, *72*, 680–686. [CrossRef]
36. Shuaib, M.; Abdulhamid, S.M.; Adebayo, O.S.; Osho, O.; Idris, I.; Alhassan, J.K.; Rana, N. Whale optimization algorithm-based email spam feature selection method using rotation forest algorithm for classification. *SN Appl. Sci.* **2019**, *1*, 390. [CrossRef]
37. Al-dhawi, B.N.S.; Kutty, S.R.M.; Baloo, L.; Almahbashi, N.M.Y.; Ghaleb, A.A.S.; Jagaba, A.H.; Kumar, V.; Saeed, A.A.H. Treatment of synthetic wastewater by using submerged attached growth media in continuous activated sludge reactor system. *Int. J. Sustain. Build. Technol. Urban Dev.* **2022**, *13*, 2–10.
38. Almahbashi, N.; Kutty, S.; Ayoub, M.; Noor, A.; Salihi, I.; Al-Nini, A.; Jagaba, A.; Aldhawi, B.; Ghaleb, A. Optimization of Preparation Conditions of Sewage sludge based Activated Carbon. *Ain Shams Eng. J.* **2020**, *12*, 1175–1182. [CrossRef]
39. Birniwa, A.H.; Kehili, S.; Ali, M.; Musa, H.; Ali, U.; Kutty, S.R.M.; Jagaba, A.H.; Abdullahi, S.S.; Tag-Eldin, E.M.; Mahmud, H.N.M.E. Polymer-Based Nano-Adsorbent for the Removal of Lead Ions: Kinetics Studies and Optimization by Response Surface Methodology. *Separations* **2022**, *9*, 356. [CrossRef]
40. Yaro, N.S.A.; Napiah, M.; Sutanto, M.H.; Usman, A.; Jagaba, A.H.; Umar, A.M.; Ahmad, A. Geopolymer utilization in the pavement industry-An overview. In *IOP Conference Series: Earth and Environmental Science, Proceedings of the 6th International Conference on Civil and Environmental Engineering for Sustainability (IConCEES 2021), Online, 15–16 November, 2021*; IOP Publishing: Bristol, UK, 2022; p. 012025.
41. Saeed, A.A.H.; Harun, N.Y.; Sufian, S.; Bilad, M.R.; Zakaria, Z.Y.; Jagaba, A.H.; Ghaleb, A.A.S.; Mohammed, H.G. Pristine and magnetic kenaf fiber biochar for Cd^{2+} adsorption from aqueous solution. *Int. J. Environ. Res. Public Health* **2021**, *18*, 7949. [CrossRef]
42. Hajialigol, S.; Masoum, S. Optimization of biosorption potential of nano biomass derived from walnut shell for the removal of Malachite Green from liquids solution: Experimental design approaches. *J. Mol. Liq.* **2019**, *286*, 110904. [CrossRef]
43. Yaro, N.S.A.; Sutanto, M.H.; Habib, N.Z.; Napiah, M.; Usman, A.; Muhammad, A. Comparison of Response Surface Methodology and Artificial Neural Network approach in predicting the performance and properties of palm oil clinker fine modified asphalt mixtures. *Constr. Build. Mater.* **2022**, *324*, 126618. [CrossRef]
44. Ugraskan, V.; Isik, B.; Yazici, O. Adsorptive removal of methylene blue from aqueous solutions by porous boron carbide: Isotherm, kinetic and thermodynamic studies. *Chem. Eng. Commun.* **2022**, *209*, 1111–1129. [CrossRef]
45. Rosli, M.A.; Daud, Z.; Ridzuan, M.B.; Aziz, N.A.A.; Awang, H.B.; Adeleke, A.O.; Hossain, K.; Ismail, N. Equilibrium isotherm and kinetic study of the adsorption of organic pollutants of leachate by using micro peat-activated carbon composite media. *Desalination Water Treat.* **2019**, *160*, 185–192. [CrossRef]
46. Chu, K.H. Revisiting the Temkin isotherm: Dimensional inconsistency and approximate forms. *Ind. Eng. Chem. Res.* **2021**, *60*, 13140–13147. [CrossRef]
47. Shimizu, T.; Abe, M.; Noguchi, M.; Yamasaki, A. Removal of Borate Ions from Wastewater Using an Adsorbent Prepared from Waste Concrete (PAdeCS). *ACS Omega* **2022**, *7*, 35545–35551. [CrossRef] [PubMed]
48. Jagaba, A.H.; Kutty, S.R.M.; Lawal, I.M.; Aminu, N.; Noor, A.; Al-Dhawi, B.N.S.; Usman, A.K.; Batari, A.; Abubakar, S.; Birniwa, A.H.; et al. Diverse sustainable materials for the treatment of petroleum sludge and remediation of contaminated sites: A review. *Clean. Waste Syst.* **2022**, *2*, 100010. [CrossRef]
49. Sun, Q.; Li, J.; Wang, J. Effect of borate concentration on solidification of radioactive wastes by different cements. *Nucl. Eng. Des.* **2011**, *241*, 4341–4345. [CrossRef]
50. Kankia, M.U.; Baloo, L.; Danlami, N.; Mohammed, B.S.; Haruna, S.; Abubakar, M.; Jagaba, A.H.; Sayed, K.; Abdulkadir, I.; Salihi, I.U. Performance of Fly Ash-Based Inorganic Polymer Mortar with Petroleum Sludge Ash. *Polymers* **2021**, *13*, 4143. [CrossRef]
51. Gao, P.; Yin, Z.; Feng, L.; Liu, Y.; Du, Z.; Duan, Z.; Zhang, L. Solvothermal synthesis of multiwall carbon nanotubes/BiOI photocatalysts for the efficient degradation of antipyrine under visible light. *Environ. Res.* **2020**, *185*, 109468. [CrossRef]
52. Venkatesan, J.; Ryu, B.; Sudha, P.; Kim, S.-K. Preparation and characterization of chitosan–carbon nanotube scaffolds for bone tissue engineering. *Int. J. Biol. Macromol.* **2012**, *50*, 393–402. [CrossRef]
53. Yaro, N.S.A.; Bin Napiah, M.; Sutanto, M.H.; Usman, A.; Saeed, S.M. Modeling and optimization of mixing parameters using response surface methodology and characterization of palm oil clinker fine modified bitumen. *Constr. Build. Mater.* **2021**, *298*, 123849. [CrossRef]
54. Mei, X.; Wang, J.; Yang, R.; Yan, Q.; Wang, Q. Synthesis of Pt doped Mg–Al layered double oxide/graphene oxide hybrid as novel NO x storage–reduction catalyst. *RSC Adv.* **2015**, *5*, 78061–78070. [CrossRef]
55. Jagaba, A.H.; Kutty, S.R.M.; Noor, A.; Birniwa, A.H.; Affam, A.C.; Lawal, I.M.; Kankia, M.U.; Kilaco, A.U. A systematic literature review of biocarriers: Central elements for biofilm formation, organic and nutrients removal in sequencing batch biofilm reactor. *J. Water Process Eng.* **2021**, *42*, 102178. [CrossRef]

56. Li, X.; Zhang, D.; Xiang, K.; Huang, G. Synthesis of polyborosiloxane and its reversible physical crosslinks. *RSC Adv.* **2014**, *4*, 32894–32901. [CrossRef]
57. Ullah, S.; Bustam, M.A.; Al-Sehemi, A.G.; Assiri, M.A.; Kareem, F.A.A.; Mukhtar, A.; Ayoub, M.; Gonfa, G. Influence of post-synthetic graphene oxide (GO) functionalization on the selective CO_2/CH_4 adsorption behavior of MOF-200 at different temperatures; an experimental and adsorption isotherms study. *Microporous Mesoporous Mater.* **2020**, *296*, 110002. [CrossRef]
58. Nekhunguni, P.M.; Tavengwa, N.T.; Tutu, H. Sorption of uranium (VI) onto hydrous ferric oxide-modified zeolite: Assessment of the effect of pH, contact time, temperature, selected cations and anions on sorbent interactions. *J. Environ. Manag.* **2017**, *204*, 571–582. [CrossRef]
59. Jagaba, A.H.; Kutty, S.R.M.; Baloo, L.; Hayder, G.; Birniwa, A.H.; Taha, A.T.B.; Mnzool, M.; Lawal, I.M. Waste Derived Biocomposite for Simultaneous Biosorption of Organic Matter and Nutrients from Green Straw Biorefinery Effluent in Continuous Mode Activated Sludge Systems. *Processes* **2022**, *10*, 2262. [CrossRef]
60. Mahato, J.K.; Gupta, S.K. Exceptional adsorption of different spectral indices of natural organic matter (NOM) by using cerium oxide nanoparticles (CONPs). *Environ. Sci. Pollut. Res.* **2021**, *28*, 45496–45505. [CrossRef]
61. Ghaleb, A.A.S.; Kutty, S.R.M.; Ho, Y.-C.; Jagaba, A.H.; Noor, A.; Al-Sabaeei, A.M.; Almahbashi, N.M.Y. Response surface methodology to optimize methane production from mesophilic anaerobic co-digestion of oily-biological sludge and sugarcane bagasse. *Sustainability* **2020**, *12*, 2116. [CrossRef]
62. Radhwan, H.; Shayfull, Z.; Farizuan, M.R.; Effendi, M.S.M.; Irfan, A.R. Optimization parameter effects on the quality surface finish of the three-dimensional printing (3D-printing) fused deposition modeling (FDM) using RSM. *AIP Conf. Proc.* **2019**, *2129*, 020155. [CrossRef]
63. Jagaba, A.H.; Kutty, S.R.M.; Abubakar, S.; Birniwa, A.H.; Lawal, I.M.; Umaru, I.; Usman, A.K.; Yaro, N.S.A.; Al-Zaqri, N.; Al-Maswari, B.M.; et al. Synthesis, Characterization, and Performance Evaluation of Hybrid Waste Sludge Biochar for COD and Color Removal from Agro-Industrial Effluent. *Separations* **2022**, *9*, 258. [CrossRef]
64. Wang, Z.; Jia, Y.; Liu, X.; Liao, L.; Wang, Z.; Wang, Z. Removal of boron in desalinated seawater by magnetic metal-organic frame-based composite materials: Modeling and optimizing based on methodologies of response surface and artificial neural network. *J. Mol. Liq.* **2022**, *349*, 118090. [CrossRef]
65. Xue, S.; Tan, J.; Ma, X.; Xu, Y.; Wan, R.; Tao, H. Boron-doped activated carbon derived from Zoysia sinica for Rhodamine B adsorption: The crucial roles of defect structures. *Flatchem* **2022**, *34*, 100390. [CrossRef]
66. Goren, A.; Okten, H. Energy production from treatment of industrial wastewater and boron removal in aqueous solutions using microbial desalination cell. *Chemosphere* **2021**, *285*, 131370. [CrossRef] [PubMed]
67. Jagaba, A.H.; Kutty, S.R.M.; Naushad, M.; Lawal, I.M.; Noor, A.; Affam, A.C.; Birniwa, A.H.; Abubakar, S.; Soja, U.B.; Abioye, K.J.; et al. Removal of nutrients from pulp and paper biorefinery effluent: Operation, kinetic modelling and optimization by response surface methodology. *Environ. Res.* **2022**, *214*, 114091. [CrossRef] [PubMed]
68. Guan, L.; Huang, C.; Han, D.; Zhu, L.; Mei, Y.; He, D.; Zu, Y. Reaction pathways of n-butane cracking over the MFI, FER and TON zeolites: Influence of regional differences in Brønsted acid sites. *Microporous Mesoporous Mater.* **2022**, *330*, 111605. [CrossRef]
69. Lawal, I.M.; Bertram, D.; White, C.J.; Jagaba, A.H.; Hassan, I.; Shuaibu, A. Multi-criteria performance evaluation of gridded precipitation and temperature products in data-sparse regions. *Atmosphere* **2021**, *12*, 1597. [CrossRef]
70. Pareek, P.; Yu, W.; Nguyen, H.D. Optimal Steady-State Voltage Control Using Gaussian Process Learning. *IEEE Trans. Ind. Inform.* **2020**, *17*, 7017–7027. [CrossRef]
71. Yaro, S.N.A.; Sutanto, M.H.; Usman, A.; Jagaba, A.H.; Sakadadi, M.Y. The influence of waste rice straw ash as surrogate filler for asphalt concrete mixtures. *Construction* **2022**, *2*, 118–125. [CrossRef]
72. Duran, H.; Yavuz, E.; Sismanoglu, T.; Senkal, B. Functionalization of gum arabic including glycoprotein and polysaccharides for the removal of boron. *Carbohydr. Polym.* **2019**, *225*, 115139. [CrossRef]
73. Jagaba, A.H.; Kutty, S.R.M.; Noor, A.; Affam, A.C.; Ghfar, A.A.; Usman, A.K.; Lawal, I.M.; Birniwa, A.H.; Kankia, M.U.; Afolabi, H.K.; et al. Parametric optimization and kinetic modelling for organic matter removal from agro-waste derived paper packaging biorefinery wastewater. *Biomass-Convers. Biorefinery* **2022**, 1–18. [CrossRef]
74. Azimi, E.B.; Badiei, A.; Ghasemi, J.B. Efficient removal of malachite green from wastewater by using boron-doped mesoporous carbon nitride. *Appl. Surf. Sci.* **2018**, *469*, 236–245. [CrossRef]
75. Tatarchuk, T.; Shyichuk, A.; Mironyuk, I.; Naushad, M. A review on removal of uranium(VI) ions using titanium dioxide based sorbents. *J. Mol. Liq.* **2019**, *293*, 111563. [CrossRef]
76. Birniwa, A.H.; Abubakar, A.S.; Huq, A.O.; Mahmud, H.N.M.E. Polypyrrole-polyethyleneimine (PPy-PEI) nanocomposite: An effective adsorbent for nickel ion adsorption from aqueous solution. *J. Macromol. Sci. Part A Pure Appl. Chem.* **2021**, *58*, 206–217. [CrossRef]
77. Chen, X.; Hossain, F.; Duan, C.; Lu, J.; Tsang, Y.F.; Islam, S.; Zhou, Y. Isotherm models for adsorption of heavy metals from water—A review. *Chemosphere* **2022**, *307*, 135545. [CrossRef] [PubMed]